Int. J. Electrochem. Sci., 17 **(2022)** Article Number: 22014, doi: 10.20964/2022.01.24

International Journal of ELECTROCHEMICAL SCIENCE
www.electrochemsci.org

Short Communication

Investigation of Long-term Corrosion of AA2024 and AA5119 Aluminum Alloys under chromate coating in Marine Atmosphere by Electrochemical Impedance Technology

Yan Li

Department of Pharmacy and Health Management, Hebei Chemical & Pharmaceutical College, Shijiazhuang 050026, China
E-mail: YanLi2021@protonmail.com

Received: 18 August 2021/ *Accepted:* 17 September 2021 / *Published:* 6 December 2021

This study was focused on the long-term corrosion performance of coated AA2024 and AA5119 aluminum alloys in the atmosphere and coastal environment after 4, 8 and 12 years of exposure. Structural analyses of samples using SEM and XRD analyses revealed that the corrosive surface area of alloys increased with increasing the atmospheric exposure time, and formation of $Al(OH)_3$ as corrosion product on the corroded surface layer of both atmospheric exposed 12 years samples. Comparison between the exposed 12 years samples showed that the higher level of impurities, deeper pits and exfoliation corrosion were observed for exposed AA2024 sample which related to the destruction of anodic oxide film due to pitting attack and decrease of protection capability of the epoxy coated layer, and lower level of impurities and corrosion on the AA5119 sample can be related to the presence of lower Si/Mg molar ratio in the alloy. Electrochemical impedance studies showed the decrease in corrosion resistance with the increase in the duration of atmospheric exposure. Results also showed that deposition of corrosion products on the surface of AA5119 alloy can act as a protective layer through preferentially filling the pores/defects. Therefore, the observations indicate the corrosion resistance of aluminum alloys is significantly dependent on the composition and created crystal defects in the manufacturing process of alloys. Coated AA5119 aluminum alloys show a higher corrosion resistance than that AA2024 in long-term atmosphere exposure in the coastal environments.

Keywords: AA2024 aluminum alloy; AA5119 aluminum alloy; Coastal environment; Long-term atmospheric corrosion; Pitting corrosion

1. INTRODUCTION

Nowadays, the composition of Aluminum alloys have been widely applied as engineering materials in the packaging food, medication, and beverages, brazing industry, cable industry, wind and solar energy management, and marine shipbuilding, automobile and aerospace industries because of its

special characteristics such as lightness, high strength and flexibility, high processability, low density, excellent corrosion resistance, high thermal stability and specific stiffness, eco-friendly nature [1, 2].

However, long-term exposure to the atmosphere, humidity and corrosive environments is a major concern because it can lead to severe corrosion of the external surfaces, with the consequent risk of breakdowns or in extreme cases structural [3-5]. Currently, insufficient and relatively sparse studies have been conducted on long-term corrosion in corrosive environments such as marine and industrial environments with a high level of chloride, humidity and pollution [6-8]. Moreover, some effects of corrosive factors such as harsh climate and pollutant impurities, extreme weather changes, dust and atmospheric contaminants need to be studied in the long term [9-11]. Thus, the long-term corrosion of aluminum alloys is the major problem in aerospace, automotive, shipbuilding and biomedical industries [12, 13].

Therefore, evaluation the long-term corrosion behavior of aluminum alloys in coastal environments is essential significance to optimize the manufacturing method and composition of aluminum alloy for engineering material applications [14, 15]. Few studies have been conducted on the long term corrosion of aluminum alloys [3, 16-20], especially for series 2 and series 5 of aluminum alloys and comparison between them has not been perfectly studied. Furthermore, among the analytical methods, electrochemical corrosion techniques as interesting and low-cost techniques can use for the study of corrosion properties of aluminum alloys. Therefore, this study was focused on long-term corrosion performance of AA2024 and AA5119 aluminum alloys in the atmosphere in coastal environment.

2. MATERIALS AND METHOD

2.1. Samples and exposure experiments

Extruded sheet of AA2024 and AA5119 aluminum alloys (Shandong Jichang Trading Co., Ltd., China) with a 220 mm length (defined as longitudinal (L) and direction of extrusion), 400 mm width (long transverse (T)), and 4 mm thickness (as short transverse (S)) were provided as the substrate. The chemical composition of aluminum alloys is presented in Table 1. The samples were ultrasonically degreased and cleaned in acetone (≥99%, Sigma-Aldrich) for 20 minutes, dehydrated with ethanol (>99%, Merck, Germany), and then rinsed with deionized water. Subsequently, the samples were anodized in mixtures of 10wt% sulphuric (Merck, Germany) and 5 wt% boric (Merck, Germany) acids for 15 minutes under a current density of 5mA/cm^{2}to obtain the 10 ± 5μm of anodic oxide film [21, 22]. Afterward, zinc chromate (99%, Sigma-Aldrich) as an anti-corrosive primer based on the epoxy resin was air-sprayed within 12 hours, and then the samples were dried and well-ventilated at 50 °C to obtain a dry film thickness of 50 ± 4μm on samples [23].

Table 1. AA2024 and AA5119 aluminum alloys chemical composition.

Element (wt %)	Cu	Mg	Ni	Mn	Fe	Zn	Si	Cr	Ti	Others	Al
AA2024	3.8	1.57	0.001	0.3	0.5	0.25	0.50	0.1	0.15	0.05	Balance
AA5119	0.05	5.6	0.001	0.3	0.5	0.25	0.25	0.3	0.15	0.06	Balance

The exposure experiments were carried out in Qingdao atmospheric corrosion site in China. Table 2 presents the average environmental parameters during the exposure measurements in 2001 at Qingdao. The prepared AA2024 and AA5119 samples were mounted on a test rack at an angle of 45° to the horizontal and exposed to ambient air with the skyward surface facing south because the samples were highly prone to corrosion and aging. Four samples were selected from the test sites after 4, 8 and 12 years' exposure.

Table 2. Average environmental parameters and atmospheric pollutant concentrations at the Qingdao site

Air temperature (°C)	Relative humidity (%)	Rainfall precipitation (mm)	Sulfation concentration ($mg\times10^{-2}/(m^2d)$)	Sea-salt particles concentration ($mg\times10^{-2}/(m^2d)$)	H_2S concentration ($mg\times10^{-2}/(m^2d)$)
25.7	83	174	0.3287	0.5606	0.0607

2.2. Analyses

Electrochemical impedance spectroscopy (EIS) studies were conducted on the frequency range of 10^5Hz to 10^{-2}Hz at open-circuit with AC potential amplitude 20mV using *a* Potentiostat/Galvanostat (PAR EG&G Model 273A) in a three-electrode system which contained the prepared aluminum alloy samples with a coating surface area of 1 cm^2 as a working electrode, a KCl saturated Ag/AgCl electrode as a reference electrode and a platinum plate as a counter electrode. 3.5% NaCl solution was used as an electrolyte solution. The topography of surface of the prepared AA2024 and AA5119 aluminum alloy samples was analyzed with scanning electron microscope (SEM, JSM-6360LA, JEOL Ltd., Tokyo, Japan). The crystal structure of corrosion products was analyzed using X-ray diffraction (XRD; Philips X'Pert MPD; CuKα radiation, Eindhoven, the Netherlands).

3. RESULTS AND DISCUSSION

Figure 1 shows the visual appearance of as prepared coated AA2024 sample and coated AA2024 samples exposed for 4, 8 and 12 years, and coated AA5119 sample for 12 years exposed in

the Qingdao atmospheric corrosion site. As seen, the appearances of the coating changed remarkably with exposure time and the corrosion rate increased with aging time. Figure 1a shows as prepared coated AA2024 with smooth surface, and Figure 1b depicts the coated AA2024 sample exposed for 4 years no significantly change toward the as-prepared sample. As observed from Figure 1c, the small quantities of impurities and salts were generated on the sample surface after 8 years. For both of exposed 4 and 8 years samples, there is macroscopically visible intact area of the surface coating. Figures 1d and 1e for exposed 12 years coated samples of AA2024 and AA5119 show that the impurities and salts not only were generated on both of samples but also there is a small amount of sand and dust. Comparison between the exposed 12 years samples reveals that the higher levels of impurities and exfoliation corrosion are observed for exposed 12 years AA2024 sample which related to destruction of the anodic oxide film and decrease of protection capability of epoxy coated layer [24], and lower level of impurities and corrosion on the AA5119 sample can be related to the presence of lower Si/Mg molar ratio in alloy [25].

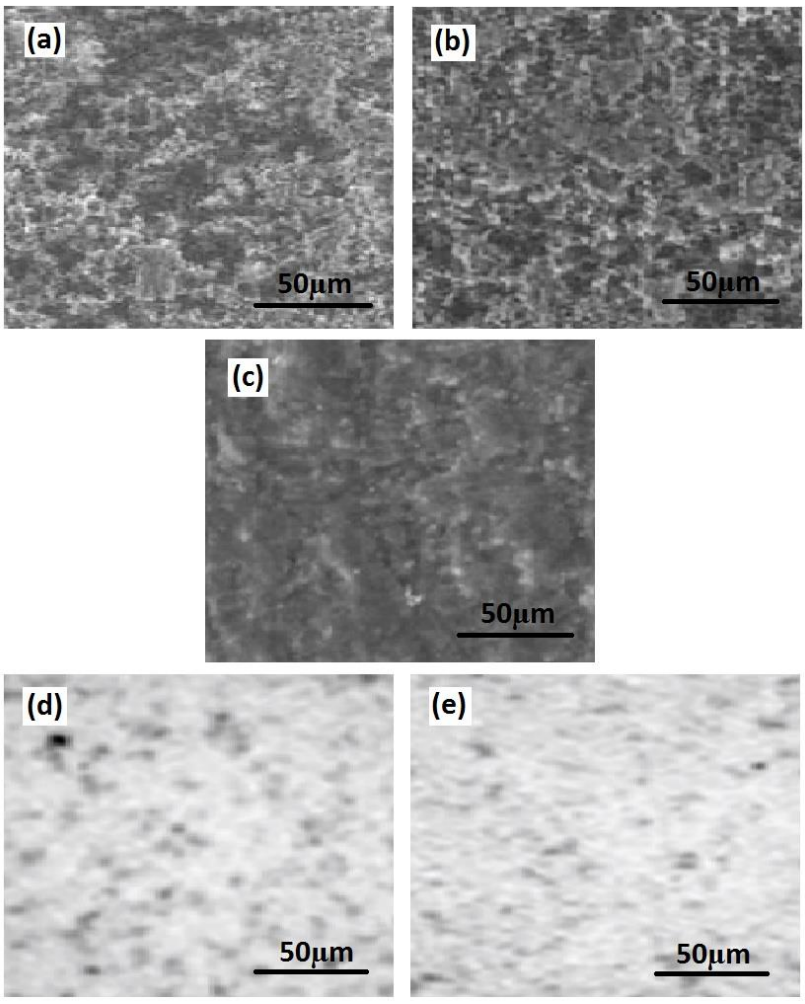

Figure 1. The visual appearance of (a) as prepared coated AA2024 sample and coated AA2024 samples exposed for (b) 4, (c) 8 and (d) 12 years, and (e) coated AA5119 sample for 12 years exposed in the Qingdao atmospheric corrosion site.

Figure 2 shows the XRD patterns of powders of corroded coated AA2024 and AA5119 samples for 12 years of atmospheric exposed that diffraction peaks reveal the presence of Al. XRD patterns of powder of corroded surface layer of both of atmospheric exposed 12 years samples display the formation of $Al(OH)_3$ in corrosion product that it causes to swell due to formation of exfoliation corrosion product, corrosive attack and corrosion products forces in grain boundaries parallel to the surface of a metal which leads to the layers apart [26]. The weak diffraction peak of $Al(OH)_3$ in XRD patterns of AA5119 sample indicates to the formation of small amounts of corrosion products on the AA5119 sample surface which is in agreement with the results of the visual appearance of AA5119 sample.

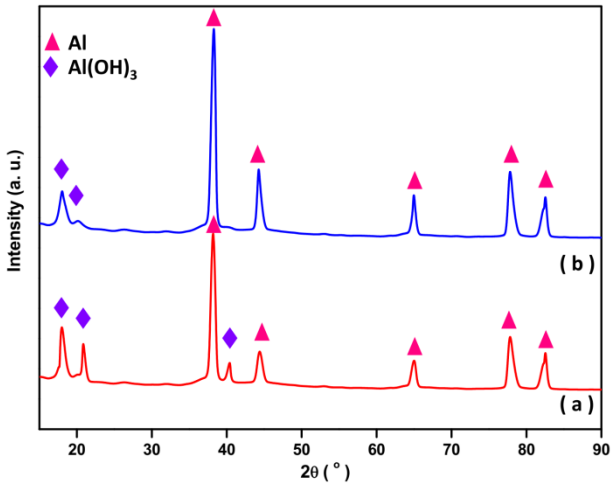

Figure 2. XRD pattern of powder of corroded surface layer of atmospheric exposed 12 years samples (a) coated AA2024 and (b) coated AA5119.

Figures 3a and 3b exhibit the obtained Bode plots of coated AA2024 samples after 4, 8 and 12 years of atmospheric exposure, and AA5119 samples after 12 years of atmospheric exposure which contain the impedance magnitude log (|Z|) and phase angle *vs.* log frequency, respectively to describe the frequency specific impedance behavior of the system.

As observed from Figure 3a, there are the diagonal lines of the impedance plots at high frequency which associated with the coating capacitance which red-shifted with the exposure time that it is interpreted as an increase in capacitance of the coating and decrease in corrosion resistance with the increase in the duration of atmospheric exposure [17, 27]. Furthermore, when the coated AA2024 samples are exposed to the coastal atmosphere for a long time, the 0.01 Hz impedance varied from 69.81 MΩ cm^2 to 0.08 MΩ cm^2. Moreover, Figure 3a shows that the slopes of lines in the middle-frequency region of Bode log |Z| plots are between −0.49 and −0.18 which is interpreted as Warburg impedance in coated samples [28]. Warburg impedance is formed due to the resistance of epoxy zinc chromate as organic films on the metal surface, indicating to the electrolyte diffuse into the pore-space between particles along the tortuous paths [28, 29].

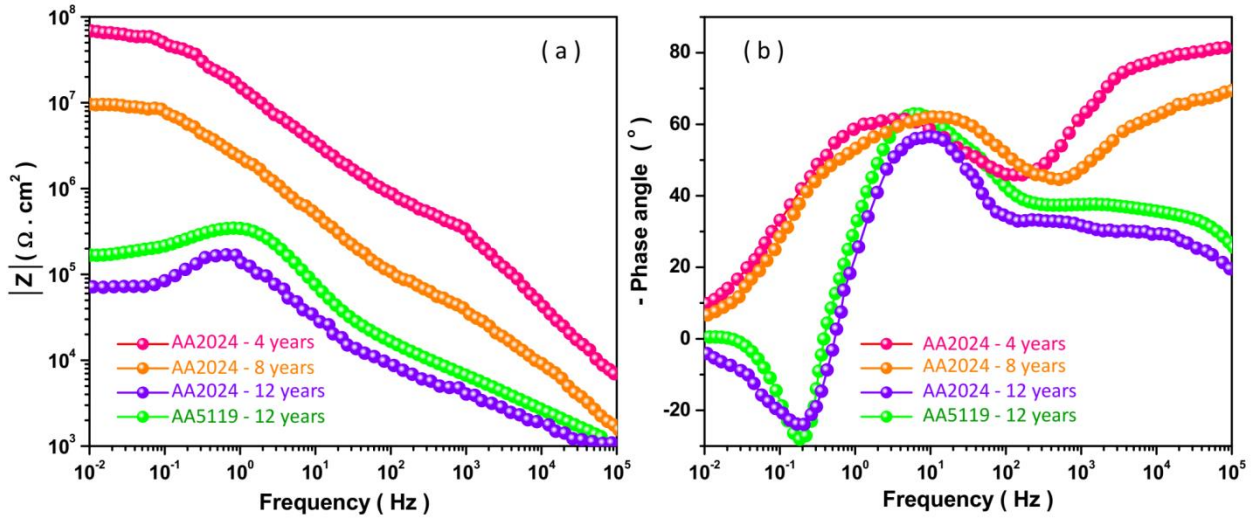

Figures 3. Bode plots of (a) log |Z| and (b) phase angle *vs.* log frequency of samples after 4, 8 and 12 years of exposure.

Furthermore, the coated AA2024 sample exposed for 12 years in Figures 3b shows the lowest phase angle value at the low-frequency region which implied to decrease of corrosion resistance of system [11]. Figure 3b also presents three-time constants for all samples that it is attributed to the three different phases, containing the corrosion of the aluminum alloy, dissolution resistance of anodic oxide layers formed on aluminum alloy, and coated epoxy resin [30].

When the chloride ions in the electrolyte diffuses the anodic oxide film surface, chloride ions facilitate the anodic dissolution of aluminum and forming chlorinated and hydro chlorinated complexes and causes a pitting attack. The mechanism of pitting corrosion by chloride ions have been suggested as follow [31]: chloride ions accumulation at the metal/film interface enhance the breakdown of the anodic film and they facilitate migration of aggressive anions to reach the metal-film interface. Rapid destruction of the anodic oxide film and formation of the intermediate chloride complex aluminum chloride is occurred at film micro-cracks (more numerous in the neighborhood of intermetallics) which constitute weak points and facilitate the localized attack. The corrosion process at the base of the pit can be described as anodic oxidation of aluminum (reaction (1)), cathodic reductions as dissolved oxygen or H^+ (reactions (2) and (3)) as following electrochemical reactions [32, 33]:

$$Al \rightarrow Al^{3+} + 3e^- \quad (1)$$

$$\frac{3}{2}O_2 + 3H_2O + 6e^- \rightarrow 6OH^- \quad (2)$$

$$6H^+ + 6e^- \rightarrow 3H_2 \quad (3)$$

The general reaction for the pitting corrosion of aluminum is presented in reaction (4) [33] which is in agreement with the results of XRD analysis:

$$2Al + 3H_2O + \frac{3}{2}O_2 \rightarrow 2Al(OH)_3 \quad (4)$$

The formation of Al^{3+} ions in anodic oxidation of aluminum (reaction (1)) at the bottom of the pitting results in the local creation of an electric field which accelerates diffuse of chloride ions to the bottom of the pitting and enhance the localized corrosion rate and formation of chlorinated and hydrochlorination complexes at the bottom of cracks according to reactions (5) to (8) [32-34].

$$Al^{3+} + 3H_2O \rightarrow Al(OH)_3 + 3H_2 \quad (5)$$
$$Al + nCl^- \rightarrow AlCl^-_n + 3e^- \quad (6)$$
$$Al + 2OH + Cl^- \rightarrow Al(OH)_2Cl + 3e^- \quad (7)$$
$$Al(OH)_2Cl + Cl^- \rightarrow Al(OH)Cl_2 + OH^- \quad (8)$$

Figure 3a indicates that after 4 and 8 years of exposure, the impedance of the coating still shows higher values, and the epoxy zinc chromate coating on these samples had a protective effect on the substrate. On the contrary, after 12 years of exposure to both AA2024 and AA5119 samples, the phase angle was less than zero at the low-frequency region (Figure 3b). This phenomenon shows the inductive characteristics [35, 36], and indicates that the coating has lost its capability of protecting the substrate [3, 37].

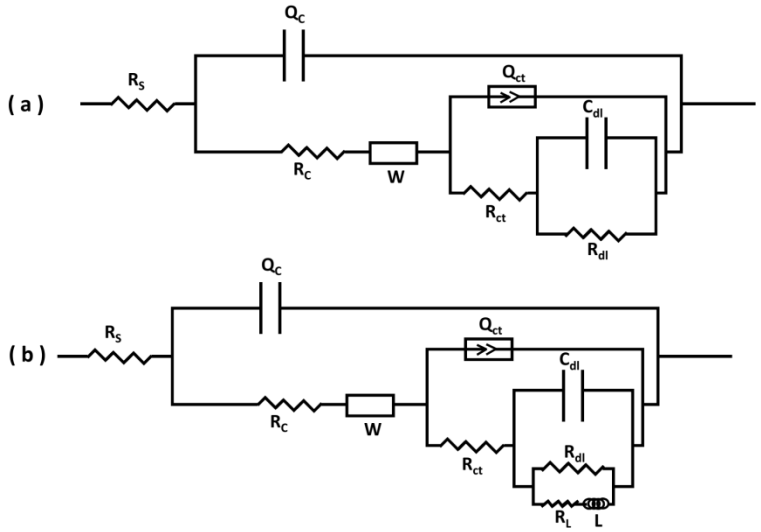

Figure 4. The equivalent circuits for fitting experimental EIS results of samples after (a) 4 and 6, and (b) 12 years of exposure.

Thus, the equivalent circuit of the samples after 4 and 8 years exposure could be different from of the samples after 12 years exposure. Figure 4 depicts the equivalent circuits for fitting experimental EIS results of coated aluminum alloys samples after 4, 8 and 12 years of exposure. Equivalent circuit elements contain the coating capacitance (Q_c), coating resistance (R_c), electrolyte solution resistance (R_s), Warburg diffusion impedance through the coating (W) which illustrates the impedance of a diffusion-controlled corrosion process [38]. Double-layer capacitance (Q_{ct}) represents the capability of the electrode to cause charge flow in the electrolyte without electron transfer [39]. Charge transfer resistance (R_{ct}) demonstrates the charge transfer process occurring on the surface of the anodic oxide film. R_{dl} and C_{dl} are two important parameters which display the charge-transfer in corrosion reaction at the aluminum alloy/electrolyte interface that their smaller values represent the more effective the

coating to prevent the corrosion reactions of the aluminum alloy surface [40]. Inductance (L) and inductive resistance (R_L) are attributed to inductive response appearing at low-frequency of corrosion process that related with the adsorption corrosion products on the metal surfaces [41, 42]. In this study, the evolution of the frequency response during corrosion reactions does not behave as an ideal capacitor, accordingly the constant phase elements Q (CPE) were used in order to fit the double layer capacitance that accounts for the non-ideal and non-homogeneous systems. Z_Q is the impedance of Q which presented as following equation [43, 44]:

$$Z_Q=Y_0^{-1}(j\omega)^{-\alpha} \quad (0 \le \alpha \le 1) \qquad (9)$$

Where Y_0 is a constant, j and ω represent the imaginary number ($j^2 = -1$) and the angular ($\omega = 2\pi f$), respectively. f is frequency, and α corresponds to the frequency power. The CPE demonstrates a pure capacitor when α = 1. Table 3 exhibits the fitted EIS results with the fit program ZSimp Win software. As seen, with the increase in the exposure time of samples the values of R_c, R_{dl} and R_{ct} are decreased which is evidence of aggressiveness of chloride ion to break the passive oxide film on aluminum alloys that it initiates to cause localized corrosion and destruction of the anodic oxide film in long term. It can be observed that the inductive resistance of the samples after 12 years of exposure are obtained 6.99×10^4 and 7.58×10^4 Ω cm^2 for coated AA2024 and AA5119, respectively, illustrating deposition of corrosion products on the surface of alloy which can act as a protective layer through preferentially filling the pores/defects [17]. The accumulated corrosion products form a dome shape on the top of the pits and gradually cover the pits and block the shallow corrosion holes which hindered the ion exchange between the electrolyte and inside the holes [45]. A higher value of inductive resistance is obtained for coated AA5119 sample reveals that the corrosion products deposited on the surface of coated AA5119 sample is effectively protected the aluminum alloy substrate because of lower Si/Mg molar ratios that that AA2024 [46, 47]. Attack from chloride ions can be aggravated in grain boundaries and crystalline defects such as Mg_2Si and $MgCl_2$ precipitates which penetrate deep into the matrix of aluminum alloy poses [34, 48].

Table 3. The fitted EIS results

Samples	Q_c (nF cm^{-2})	n_c	R_c (MΩ cm^2)	Q_{ct} (nF cm^{-2})	n_f	R_{ct} (MΩ cm^2)	C_{dl} (nF cm^{-2})	R_{dl} (MΩ cm^2)	R_l (Ω cm^2)	L (H) × 10^4
AA2024 - 4 years	1.02	0.89	0.681	12.3	0.75	23.901	2.60	45.97	0.002	
AA2024 - 8 years	26.32	0.75	0.087	45.9	0.79	4.951	86.19	5.41	0.001	
AA2024 - 12 years	949.1	0.60	0.007	209.8	0.90	0.015	204.99	0.25	6.99×10^4	9.97
AA5119 - 12 years	890.3	0.63	0.008	193.2	0.88	0.081	189.54	0.97	7.58×10^4	12.4

The SEM micrographs of as prepared coated AA2024 sample, and coated AA2024 samples exposed for 4, 8 and 12 years, and coated AA5119 samples exposed for 12 years are shown in Figure 5. It is found from images that the corrosive surface area of alloys increases with increasing the atmospheric exposure time. As seen, the created pits exhibit the crystallographic characteristics due to hexagonal prismatic cell structure of aluminum and anodic aluminum oxide film [49]. Moreover, coated AA2024 sample exposed for 12 years shows multiple corrosion defects and deeper pits and

more interlinked inner pits than AA5119 sample that these facilitate the formation of transport tunnels for aggressive chloride ions and corrosive substances which increase corrosion rate [16].

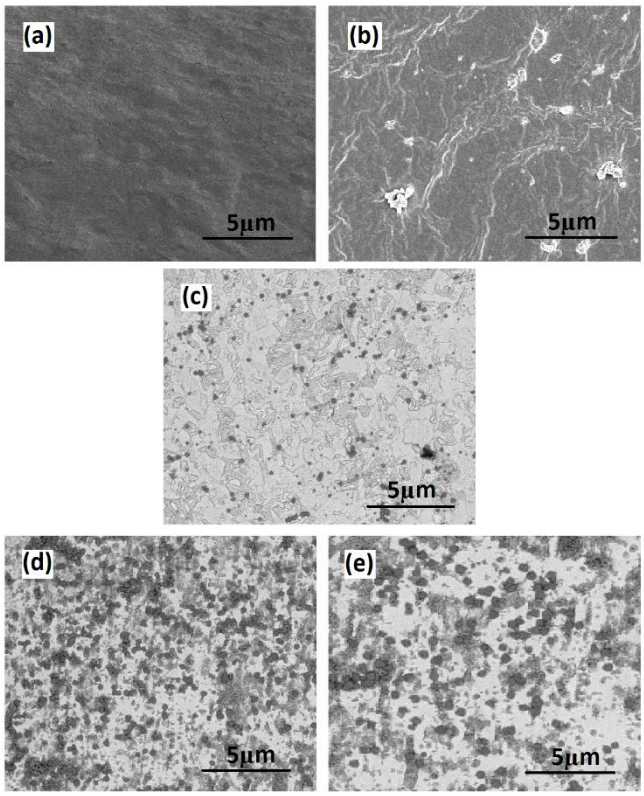

Figure 5. The SEM micrographs of (a) as prepared coated AA2024 sample, and coated AA2024 samples exposed for (b) 4, (c) 8 and (d) 12 years, and (e) coated AA5119 sample exposed for 12 years.

4. CONCULUSION

This study presented the long term corrosion behavior of coated AA2024 and AA5119 aluminum alloys in the atmosphere in the coastal environment at the Qingdao test site after 4, 8 and 12 years of exposure. Structural results showed that corrosive surface area of alloys increased with increasing the atmospheric exposure time. Comparison between the exposed 12 years samples revealed that the higher level of impurities, deeper pits and more $Al(OH)_3$ as corrosion products were observed for exposed AA2024 samples which related to destruction of anodic oxide film due to pitting attack and decrease of protection capability of epoxy coated layer due to its higher Si/Mg molar ratio in AA2024 composition than that AA5119 alloy which facilitates the chloride ions attack in grain boundaries and crystalline defects such as Mg_2Si and $MgCl_2$. Moreover, coated AA2024 sample exposed for 12 years showed multiple corrosion defects and deeper pits and more interlinked inner pits than the AA5119 sample that facilitate the formation of transport tunnels for aggressive chloride ions and corrosive substances which increase corrosion rate. Results of electrochemical studies showed a decrease in corrosion resistance with the increase in duration of atmospheric exposure. Results indicated the formation of three different corrosion phases, containing the corrosion of the aluminum

alloy, dissolution resistance of anodic oxide layers formed on aluminum alloy, and coated epoxy resin. Results also showed that deposition of corrosion products on the surface of AA5119 alloy can act as a protective layer through preferentially filling the pores/defects. Therefore, the observations indicate the corrosion resistance of aluminum alloys is significantly dependent on the composition and created crystal defects in the manufacturing process of alloys. Coated AA5119 aluminum alloys show a higher corrosion resistance than that AA2024 in long-term atmosphere exposure in the coastal environments.

ACKNOWLEDGEMENT
This work was sponsored in part by the National Natural Science Foundation of China (No. 21576067).

References

1. D. Varshney and K. Kumar, *Ain Shams Engineering Journal*, 12 (2021) 1143.
2. J. Xie, Y. Chen, L. Yin, T. Zhang, S. Wang and L. Wang, *Journal of Manufacturing Processes*, 64 (2021) 473.
3. T. Zhang, T. Zhang, Y. He, S. Zhang, B. Ma and Z. Gao, *Coatings*, 11 (2021) 237.
4. Y. Li, D.D. Macdonald, J. Yang, J. Qiu and S. Wang, *Corrosion Science*, 163 (2020) 108280.
5. N. Naderi, M. Hashim, J. Rouhi and H. Mahmodi, *Materials science in semiconductor processing*, 16 (2013) 542.
6. R. Zhao, L. Zhang, B. Guo, Y. Chen, G. Fan, Z. Jin, X. Gua and J. Zhu, *Composites Part B: Engineering*, 222 (2021) 109092.
7. L. Zhang, M. Zhang, S. You, D. Ma, J. Zhao and Z. Chen, *Science of The Total Environment*, 780 (2021) 146505.
8. Y. Yu, Y. Zhao, Y.-L. Qiao, Y. Feng, W.-L. Li and W.-D. Fei, *Journal of Materials Science & Technology*, 84 (2021) 10.
9. D. Knotkova and K. Kreislova, *WIT Transactions on State of the Art in Science and Engineering*, 28 (2007) 107.
10. X. Li, T. Shi, B. Li, X. Chen, C. Zhang, Z. Guo and Q. Zhang, *Materials & Design*, 183 (2019) 108152.
11. R. Mohamed, J. Rouhi, M.F. Malek and A.S. Ismail, *International Journal of Electrochemical Science*, 11 (2016) 2197.
12. X. Zhang, Y. Tang, F. Zhang and C.S. Lee, *Advanced Energy Materials*, 6 (2016) 1502588.
13. X. Guo, C. Zhang, Q. Tian and D. Yu, *Materials Today Communications*, 26 (2021) 102007.
14. H. Guan, S. Huang, J. Ding, F. Tian, Q. Xu and J. Zhao, *Acta Materialia*, 187 (2020) 122.
15. L. Zhang, J. Zheng, S. Tian, H. Zhang, X. Guan, S. Zhu, X. Zhang, Y. Bai, P. Xu and J. Zhang, *Journal of Environmental Sciences*, 91 (2020) 212.
16. T. Zhang, Y. He, R. Cui and T. An, *Journal of Materials Engineering and Performance*, 24 (2015) 2764.
17. H.-S. Lee, J.K. Singh, M.A. Ismail, C. Bhattacharya, A.H. Seikh, N. Alharthi and R.R. Hussain, *Scientific Reports*, 9 (2019) 3399.
18. Q. Zhao, C. Guo, K. Niu, J. Zhao, Y. Huang and X. Li, *Journal of Materials Research and Technology*, 12 (2021) 1350.
19. S. Zhang, T. Zhang, Y. He, X. Du, B. Ma and T. Zhang, *International Journal of Fatigue*, 129 (2019) 105225.
20. S. Sun, Q. Zheng, D. Li, J. Chen and J. Wen, *Journal of Chinese Society for Corrosion and protection*, 29 (2009)

21. L. Domingues, J. Fernandes, M.D.C. Belo, M. Ferreira and L. Guerra-Rosa, *Corrosion Science*, 45 (2003) 149.
22. Y. Sepulveda, M. Paez, J. Zagal, J. Henriquez, J. Pavez, A. Monsalve, O. Bustos and G. Thompson, *Boletín de la Sociedad Chilena de Química*, 46 (2001) 399.
23. J.M. Vega, N. Granizo, J. Simancas, D. de la Fuente, I. Díaz and M. Morcillo, *Journal of Coatings Technology and Research*, 10 (2013) 209.
24. M. Paz Martínez-Viademonte, S.T. Abrahami, T. Hack, M. Burchardt and H. Terryn, *Coatings*, 10 (2020) 1106.
25. C. Do Lee, C.S. Kang and K.S. Shin, *Metals and Materials*, 6 (2000) 441.
26. Z. Cui, X. Li, K. Xiao, C. Dong, L. Wang, D. Zhang and Z. Liu, *Journal of Materials Engineering and Performance*, 24 (2015) 296.
27. H.-S. Lee, J.K. Singh, M.A. Ismail and C. Bhattacharya, *Metals*, 6 (2016) 55.
28. J. Zhang, J. Hu, J. Zhang and C. Cao, *Progress in Organic Coatings*, 49 (2004) 293.
29. A.M.A. Alsamuraee and H.I. Jaafer, *American Journal of Scientific and Industrial Research* 2(2011) 761.
30. S.T. Abrahami, J.M. de Kok, V.C. Gudla, R. Ambat, H. Terryn and J.M. Mol, *npj Materials Degradation*, 1 (2017) 1.
31. A. Mazhar, S. Arab and E. Noor, *Journal of applied electrochemistry*, 31 (2001) 1131.
32. Febrianto, Sriyono, E.P. Hastuti and G.R. Sunaryo, *Journal of Physics: Conference Series*, 1198 (2019) 022061.
33. R. Grilli, M.A. Baker, J.E. Castle, B. Dunn and J.F. Watts, *Corrosion Science*, 52 (2010) 2855.
34. S. Adeosun, O. Sekunowo, S. Balogun and V. Obiekea, *International journal of corrosion*, 2012 (2012) 1.
35. S. Guo, J.J. Leavitt, X. Zhou, E. Lahti and J. Zhang, *RSC Advances*, 6 (2016) 44119.
36. Y. Zhang, X. Yuan, H. Huang, X. Zuo and Y. Cheng, *Materials Research Express*, 6 (2019) 0965a3.
37. G. Bierwagen, D. Tallman, J. Li, L. He and C. Jeffcoate, *Progress in organic coatings*, 46 (2003) 149.
38. N. Končan Volmajer, M. Steinbücher, P. Berce, P. Venturini and M. Gaberšček, *Coatings*, 9 (2019) 254.
39. D.R. Merrill, M. Bikson and J.G. Jefferys, *Journal of neuroscience methods*, 141 (2005) 171.
40. D. Zeng, Z. Liu, L. Zou and H. Wu, *Coatings*, 11 (2021) 842.
41. X. Yang, L. Zhang, S. Zhang, K. Zhou, M. Li, Q. He, J. Wang, S. Wu and H. Yang, *International Journal of Electrochemical Science*, 16 (2021)
42. Z. Yin, L. Liu, Y. Wang, T. Yang and Y. Chen, *International Journal of Electrochemical Science*, 15 (2020) 10825.
43. M. Yan, C. Sun, J. Xu and W. Ke, *International Journal of Electrochemical Science*, 10 (2015) 1762.
44. H. Yu, L. Ma, Z. Li and R. Jiang, *International Journal of Electrochemical Science*, 13 (2018)
45. Q. Zhang, Q. Li and X. Chen, *RSC Advances*, 11 (2021) 1332.
46. A. Pardo, M. Merino, S. Merino, M. López, F. Viejo and M. Carboneras, *Corrosion engineering, science and technology*, 39 (2004) 82.
47. A. Pardo, M. Merino, R. Arrabal, S. Merino, F. Viejo and M. Carboneras, *Surface and Coatings Technology*, 200 (2006) 2938.
48. X. Shi, G. Zhou and A. Muthumani, *Case Studies in Construction Materials*, 7 (2017) 1.
49. J.H. Seo, J.-H. Ryu and D.N. Lee, *Journal of the Electrochemical Society*, 150 (2003) B433.